01 Jan 2020

Synthesis And Characterization Of PVP Based Catalysts For Selected Application In Catalysis

Hany A. Elazab
Missouri University of Science and Technology, hany.elazab@mst.edu

Mohamed N. Ayad

Mohamed M. Hammam

Mostafa A. Radwan

et. al. For a complete list of authors, see https://scholarsmine.mst.edu/che_bioeng_facwork/1611

Recommended Citation

H. A. Elazab et al., "Synthesis And Characterization Of PVP Based Catalysts For Selected Application In Catalysis," *Biointerface Research in Applied Chemistry*, vol. 10, no. 2, pp. 5209 - 5216, BioInterface Research in Applied Chemistry, Jan 2020.
The definitive version is available at https://doi.org/10.33263/BRIAC102.209216

Volume 10, Issue 2, 2020, 5209 - 5216 ISSN 2069-5837
Biointerface Research in Applied Chemistry
www.BiointerfaceResearch.com
https://doi.org/10.33263/BRIAC102.209216
Original Research Article Open Access Journal
Received: 29.10.2019 / Revised: 20.01.2020 / Accepted: 25.01.2020 / Published on-line: 03.02.2020

Synthesis and characterization of PVP based catalysts for selected application in catalysis

Hany A. Elazab [1,2] *, Mohamed N. Ayad [1], Mohamed M. Hammam [1], Mostafa A. Radwan [1], Mohamed A. Sadek [1]
[1]Department of Chemical Engineering, Faculty of Engineering, The British University in Egypt, El-Shorouk City, Cairo, Egypt.
[2] Nanotechnology Research Centre (NTRC), the British University in Egypt (BUE), El-Sherouk City, Suez Desert Road, Cairo, 11837, Egypt
*corresponding author e-mail address: ***elazabha@vcu.edu*** | Scopus ID 57197864132

ABSTRACT
This research aims to study the catalyst activity in specific reactions and the characteristics of the catalyst in order to optimize its performance. This research investigates PVP based catalysts and their properties and applications. PVP was prepared in combination with different metal oxides in order to be tested for different catalytic applications including dye removal. Methyl orange was used as a dye and different concentrations were tested against different metallic ions in order to optimize the catalyst for being used in dye removal applications. Spectrophotometer was used to calculate the concentration of the dye before and after catalyst exposure and investigate the relation between contact time and concentrations. Applying different contact time to the same weight percent of PVP based catalyst with metallic ions revealed that increasing the contact time with a good shaking leads to decrease in the concentration of the dye mixed with the sample. The tests showed that the mixture between PVP and Nickel has the best dye removal within the other metal ions (copper and ferric) as well it showed that ferric has the least effect on dye removal. Wide angle x-ray diffraction (WA-XRD) was applied to different sample copper with PVP and ferric with PVP.
Keywords: *Dye removal, PVP, Metal oxides, catalyst, Wastewater treatment.*

1. INTRODUCTION

Textiles and waste water have dyes that could cause hazards and a lot of harm to the environment and to livings [1-5]. These dyes should be removed in order to decrease the harms by different techniques and applications used in dye removal and one of them is by PVP based catalyst mixed with different metal ions [6-12].

Polyvinyl pyrrodine PVP, which is also known polyvidone. The PVP is a polymer which is soluble in water [7-14]. This polymer contains and made of monomer called N-vinylpyrrodine [15-24]. PVP was structured and made at the first by scientist named Walter Reppe in 1939 by derivations of the acetylene [25-34]. It was first been used as a substitution for blood plasma then it started to have more and a variety of applications and uses. PVP is dissolvable in water and other polar solvents [35-46]. For instance, it is dissolvable in different alcohols, for example, ethanol and methanol, just as in progressively intriguing solvents like the profound eutectic dissolvable framed by choline chloride and urea. At the point when dry, it is a light flaky hygroscopic powder, promptly engrossing up to 40% of its load in barometrical water. In arrangement, it has brilliant wetting properties and promptly shapes films. This makes it great as a covering or an added substance to coatings [47-55].

Polyvinylpyrrolidone (PVP) having (Mw) from 2500 to around one million is for the most part gotten by radical polymerization in arrangement. The higher atomic weight type items are polymerized in watery (aquatic) arrangement generally utilizing hydrogen peroxide as initiator [56-58]. The polymers in this way acquired have hydroxyl and carbonyl end gatherings. Increasingly steady end gatherings can be acquired by polymerization in solvents, which may go about as chain exchange operators and which produce low atomic weight type items [59-61]. Copolymers particularly with monomers, for example, vinyl acetic acid derivation and with different acrylic mixes may likewise be delivered by arrangement polymerization. Popcorn polymerization prompts insoluble PVP. In this way, VP is polymerized without initiator within the sight of little measures of bifunctional monomers [64-66]. The polymeric chips therefore shaped are exceptionally cross-connected, mostly because of entrapments.

The sub-atomic weight appropriation of dissolvable PVP is expansive because of exchange responses. A bizarre property of PVP is its dissolvability in water just as in different natural solvents. The glass progress temperature of high sub-atomic weight polymers (Mw=1 million) is about 175°C and tumbles to values under 100°C with diminishing sub-atomic weight Mw=2500). PVP frames buildings with different mixes, particularly with H-benefactors, for example, phenols and carboxylic acids. The complex framed with cross-connected PVP and polyphenols is utilized economically for the elucidation of refreshments. Another business use is the complexation of iodine with straight PVP, which prompts compelling disinfectants of exceptionally low danger. Further vital utilization of PVP in the pharmaceutical field are their utilization as official or film framing specialists for tablets, and as solubilizing operators for infusions.

The swelling capacity of cross-connected PVP in water is utilized in crumbling operators for tablets. In the corrective field, PVP polymers are utilized as film formers for hair dressing items. Instances of specialized applications are glues, material helpers and scattering operators. PVP has many uses and applications most of them are used in our daily uses and others are used in the manufacturing of some huge products. One of the known and famous applications of PVP is in medical issues. It has an

important role in the pharmaceutical tablets as it is used as a binder as it has the ability to passes smoothly through the body when tablets are swallowed. Mixing PVP with iodine in order to form a compound named povidone iodine that contains antiseptic property. This compound has a widely usages as it can be used as liquid hand soaps and scrubs in surgeons. The most common name and the most widely known name which is used as daily antiseptic is Beta dine, as it has a high degree of safety, available and low cost. The PVP acts as a good lubricant that is why it can be used in eye lenses and their solutions as it can reduce the friction. As well it may be used in some eye drops products.

PVP has many other practical uses and application such as it acts as a reducing agent and distributed in NPs mixture, has a role as a stabilizer in the in organic solar cell, increase the solubility of the drugs so it can be used as an aid, can be used in gels for tooth as a thickening agent, it has an important role in agricultural process as it acts as a binder which helps in crop protection, and can be used as an additive in many products such as inkjet papers, ceramics and batteries.

2. EXPERIMENTAL SECTION

PVP dissolved on 100 ml distilled water was added to metal ions dissolved in distilled water and the mixture was stirred for 2 – 3 minutes. After mixing them well, 500 µL hydrazine hydrate was added and heated using microwave for 5 minutes using 30s intervals, then mixture was dried at oven. Methyl orange of concentration 50 ppm was prepared in distilled water using a different weight of different metallic ions adding to them methyl orange with 50 ppm concentration. Then, samples were put on the shaker for different time (10, 20, 30, 40 and 50 minutes). Finally, Spectrophotometer was used to measure the new concentrations, and a curve was drawn between the contact time and the concentrations showing the effect of contact time on concentrations.

3. RESULTS SECTION

3.1. XRD Characterization.

XRD diffraction pattern of copper chloride nanoparticles, which was prepared using microwave-assisted synthesis and characterization of (CuCl) was achieved by XRD pattern of catalyst sample as shown in figure 1. XRD of CuCl match that reference code is 01-081-1841 corresponding to cubic structure and the diffraction peaks are ascribed to the (111), (200), (220), (311), (222), and (400).

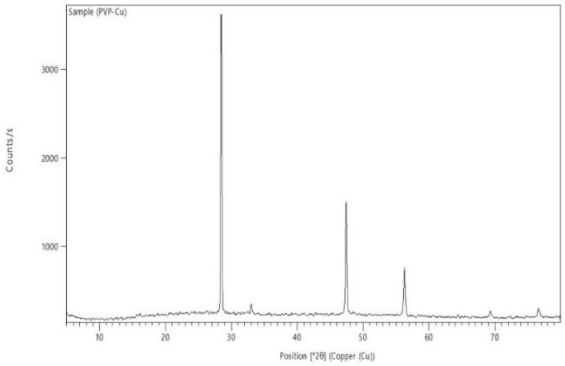

Figure 1. XRD pattern of Copper based catalyst supported on PVP.

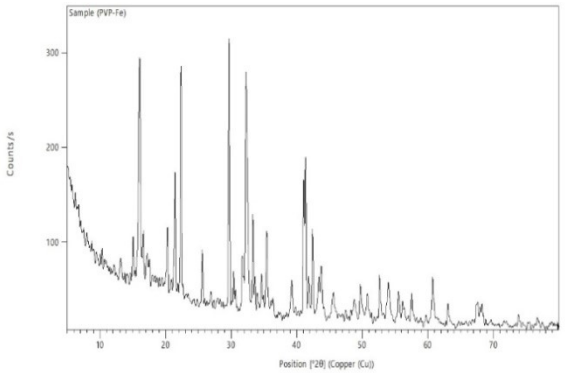

Figure 2. XRD pattern of Iron based catalyst supported on PVP.

Figure 1 displays the XRD diffraction pattern of copper chloride nanoparticles.The characterization of (CuCl) was achieved by XRD pattern of catalyst sample as we see in figure 1. XRD of CuCl match that reference code is 01-081-1841 corresponding to cubic structure and the diffraction peaks are ascribed to the (111), (440), (220), (422), (222), and (331).

Figure 2 shows the XRD diffraction of iron chloride nanoparticles and the characterization of [$FeCl_2$. $(H_2O)_4$)] was achieved by XRD of c sample as in figure 2. XRD of [$FeCl_2$. $(H_2O)_4$)] match the code is 01-071-0668 to monoclinic structure and the peaks are ascribed to the (221), (113), (110), (132), (111), (120), (300), (231) and (041).

3.2. Concentration calculations.

3.2.1. Copper Based Catalyst Supported on PVP.

Table 1 shows the concentration calculations for copper based catalyst supported on 20 wt% PVP. It is obvious that by increasing the shaking time, the concentration decreases as shown in figure 3.

Table 1. Concentration Calculations for Copper based catalyst supported on 20 wt % PVP

Shaking time/min	Abs(465nm)	Results(Conc.)
10	0.0727	0.89
20	0.0531	0.66
30	0.0463	0.58
40	0.1046	1.31
50	0.0341	0.43

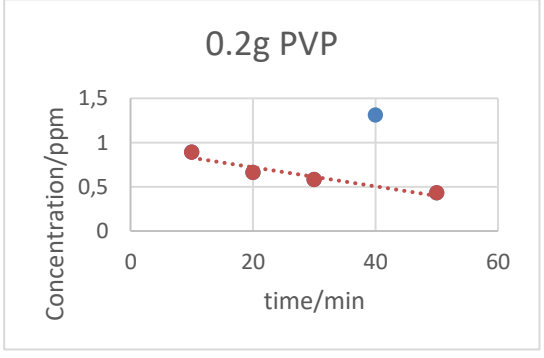

Figure 3. Effect of time on concentration of Copper based catalyst supported on PVP.

Table 2. Concentration Calculations for Copper based catalyst supported on 60 wt % PVP

Time/min.	Abs(465nm)	Results(Conc.)
10	0.1112	1.39
20	0.1271	1.59
30	0.0672	0.84
40	0.0613	0.75
50	0.0229	0.29

Table 2 shows the concentration calculations for copper based catalyst supported on 60 wt% PVP. It is obvious that by increasing the shaking time, the concentration decreases as shown in figure 4.

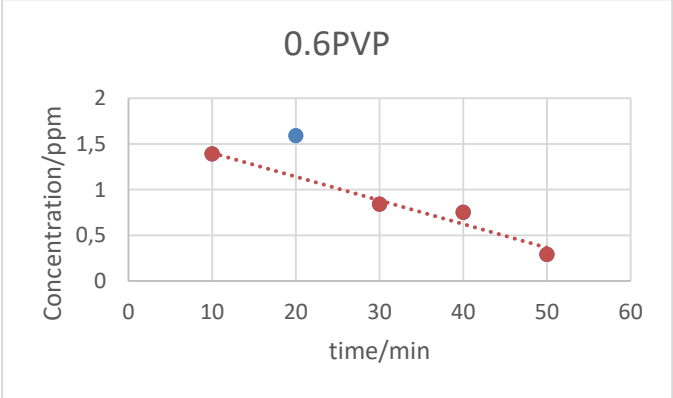

Figure 4. Effect of time on concentration of Copper based catalyst supported on PVP.

Table 3. Concentration Calculations for Copper based catalyst supported on 80 wt % PVP.

Time	Abs(465nm)	Results(Conc)
10	0.1372	1.72
20	0.1189	1.49
30	0.0995	1.24
40	0.0893	1.12
50	0.0859	1.05

Table 3 shows the concentration calculations for copper based catalyst supported on 80 wt% PVP. It is obvious that by increasing the shaking time, the concentration decreases as shown in figure 5.

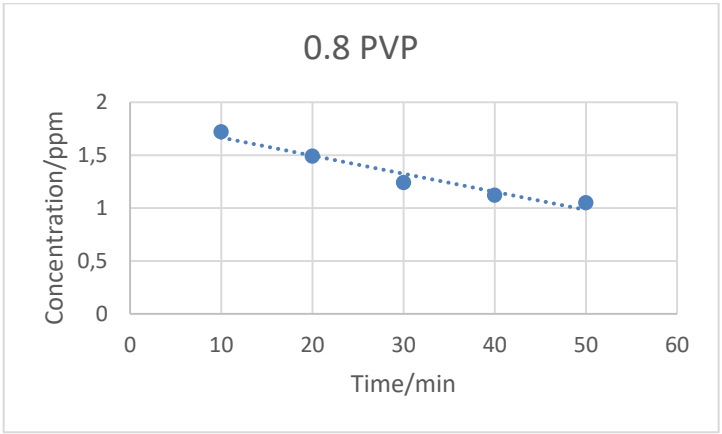

Figure 5. Effect of time on concentration of Copper based catalyst supported on PVP.

Table 4 shows the concentration calculations for copper based catalyst supported on 90 wt% PVP. It is obvious that by increasing the shaking time, the concentration decreases as shown in figure 6.

Table 4. Concentration Calculations for Copper based catalyst supported on 90 wt % PVP.

Time/min.	Abs(465nm)	Results(Conc)
10	0.1753	2.19
20	0.1418	1.77
30	0.0945	1.18
40	0.1562	1.95
50	0.0645	0.79

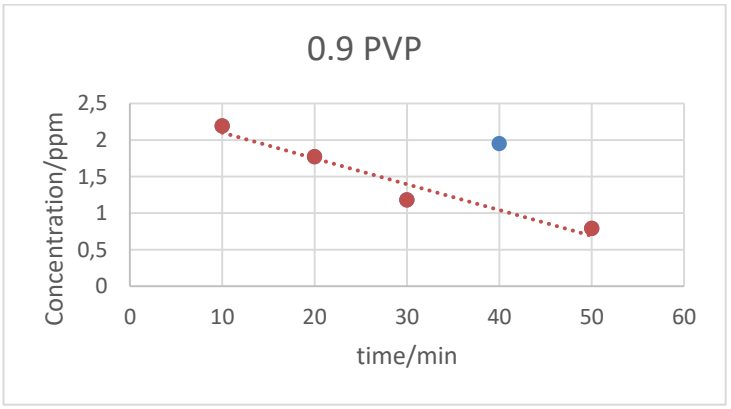

Figure 6. Effect of time on concentration of Copper based catalyst supported on PVP.

3.2.2. Iron Based Catalyst Supported on PVP.

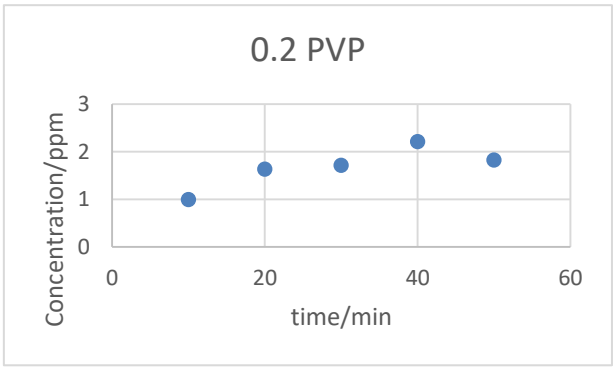

Figure 7. Effect of time on concentration of Iron based catalyst supported on PVP.

The effect of time on concentration in ppm for iron based catalyst supported on 20 wt% PVP was represented schematically as shown in Figures 7. It is obvious that by increasing the shaking time, the concentration increases in the beginning and decreases finally at 50 min. as shown in figure 7.

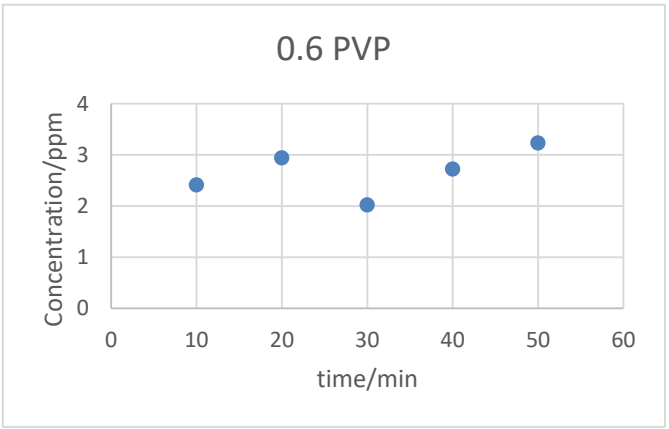

Figure 8. Effect of time on concentration of Iron based catalyst supported on 60 wt % PVP.

The effect of time on concentration in ppm for iron based catalyst supported on 60 wt% PVP was represented schematically as shown in Figures 8. It is obvious that by increasing the shaking time, the concentration decreases finally at 30 min. as shown in figure 8.

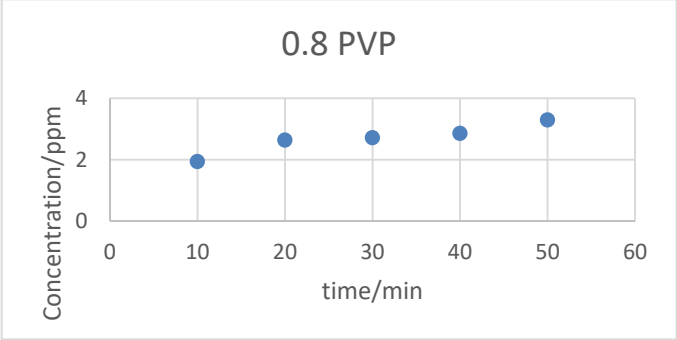

Figure 9. Effect of time on concentration of Iron based catalyst supported on 80 wt % PVP.

The effect of time on concentration in ppm for iron based catalyst supported on 80 wt% PVP was represented schematically as shown in Figures 9. It is obvious that by increasing the shaking time, the concentration is increasing. as shown in figure 9

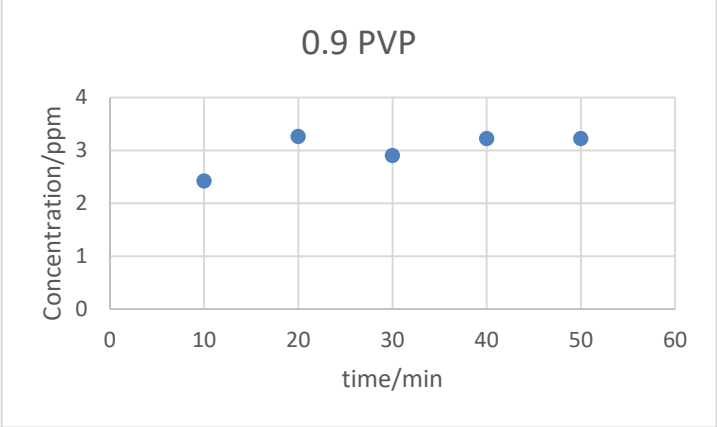

Figure 10. Effect of time on concentration of Iron based catalyst supported on 90 wt % PVP.

The effect of time on concentration in ppm for iron based catalyst supported on 90 wt% PVP was represented schematically as shown in Figures 9. It is obvious that by increasing the shaking time, the concentration is increasing. as shown in figure 10

3.2.3. Nickel Based Catalyst Supported on PVP.

Table 5. Concentration calculations for Nickel based catalyst supported on 20 wt % PVP

Time	Abs(465nm)	Concentration
10	0.4241	5.31
20	0.3654	4.57
30	0.3389	4.24
40	0.291	3.64
50	0.2839	3.55

Table 5 shows the concentration calculations for nickel based catalyst supported on 20 wt% PVP. It is obvious that by increasing the shaking time, the concentration decreases as shown in figure 11.

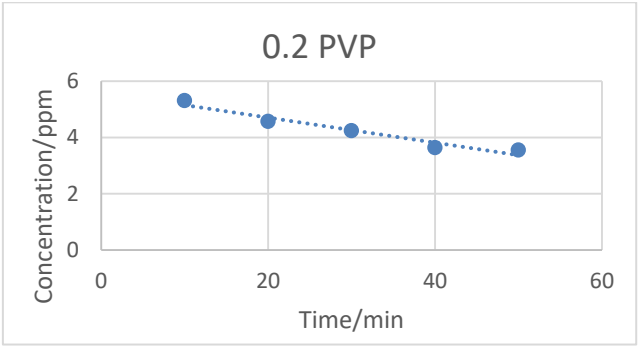

Figure 11. Effect of time on concentration of Nickel based catalyst supported on 20 wt % PVP.

Table 6. Concentration Calculations for Nickel based catalyst supported on 40 wt % PVP.

Time	Abs(465nm)	Concentration
10	0.2265	2.83
20	0.1713	2.14
30	0.0946	1.18
40	0.0709	0.89
50	0.0516	0.65

Table 6 shows the concentration calculations for nickel based catalyst supported on 40 wt% PVP. It is obvious that by increasing the shaking time, the concentration decreases as shown in figure 12.

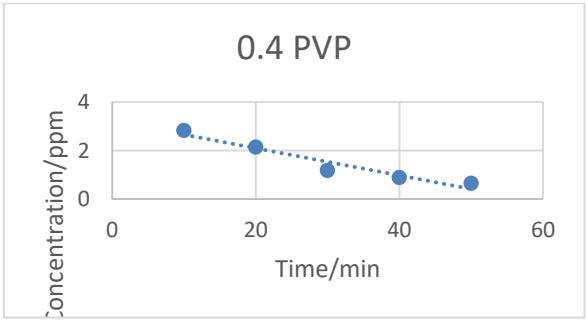

Figure 12. Effect of time on concentration of Nickel based catalyst supported on 40 wt % PVP.

Table 7. Concentration Calculations for Nickel based catalyst supported on 60 wt % PVP.

Time	Abs(465nm)	Concentration
10	0.24	3
20	0.2363	2.96
30	0.2291	2.87
40	0.2176	2.72
50	0.2457	3.07

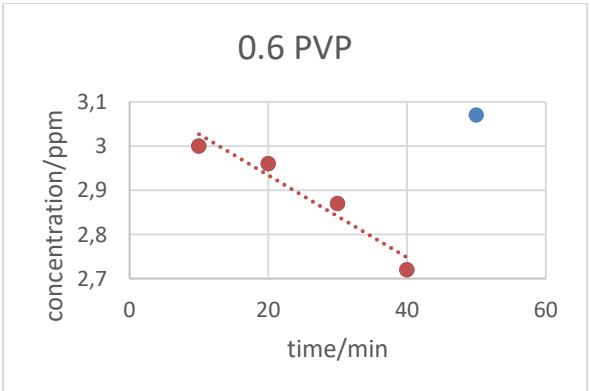

Figure 13. Effect of time on concentration of Nickel based catalyst supported on 60 wt % PVP.

Table 7 shows the concentration calculations for nickel based catalyst supported on 60 wt% PVP. It is obvious that by increasing the shaking time, the concentration decreases as shown in figure 13.

Table 8. Concentration Calculations for Nickel based catalyst supported on 80 wt % PVP.

Time/min	Abs(465nm)	Concentration
10	0.5156	6.45
20	0.4063	5.08
30	0.4088	5.11
40	0.3508	4.39
50	0.3765	4.71

Table 8 shows the concentration calculations for nickel based catalyst supported on 80 wt% PVP. It is obvious that by increasing the shaking time, the concentration decreases as shown in figure 14.

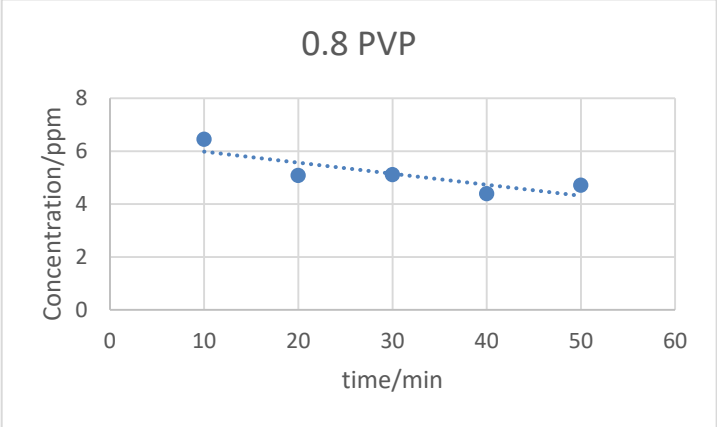

Figure 14. Effect of time on concentration of Nickel based catalyst supported on 80 wt % PVP.

Table 9. Concentration Calculations for Nickel based catalyst supported on 90 wt % PVP.

Time	Abs(465nm)	Concentration
10	1.7563	21.97
20	1.2427	15.55
30	1.6545	20.7
40	1.5204	19.02
50	1.5395	19.26

Table 9 shows the concentration calculations for nickel based catalyst supported on 90 wt% PVP. It is obvious that by increasing the shaking time, the concentration decreases as shown in figure 15.

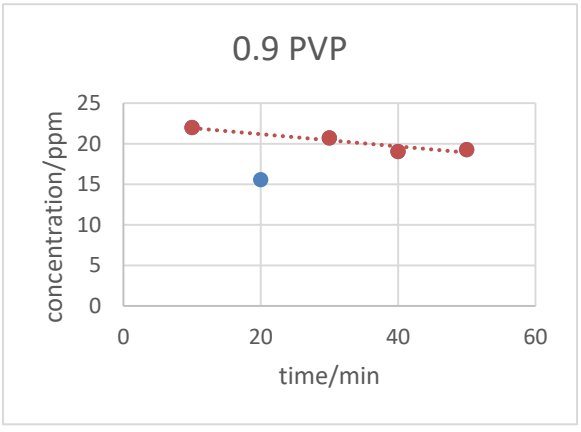

Figure 15. Effect of time on concentration of Nickel based catalyst supported on 90 wt % PVP

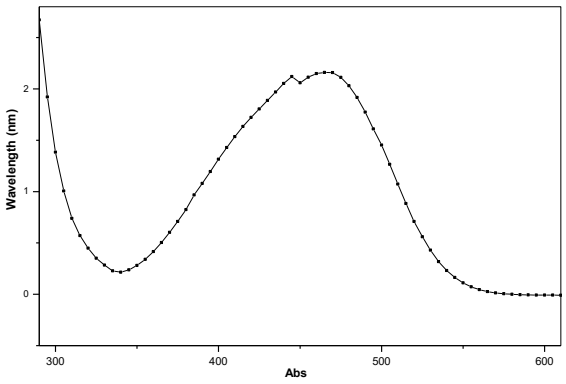

Figure 16. Wave Length Curve of Methyl Orange

In order to find the wave length of the methyl orange this curve was obtained by using the Spectrophotometer by applying the dye (methyl-orange) in the device and start to gain the reading of the wave length curve it showed that peak of the curve was 465 nm which fits with the known wave length of methyl orange in the books done by scientist as shown in figure 16. The methyl orange has been prepared with concentration 50 PPM by applying the equation MV=MV to obtain the needed concentration.

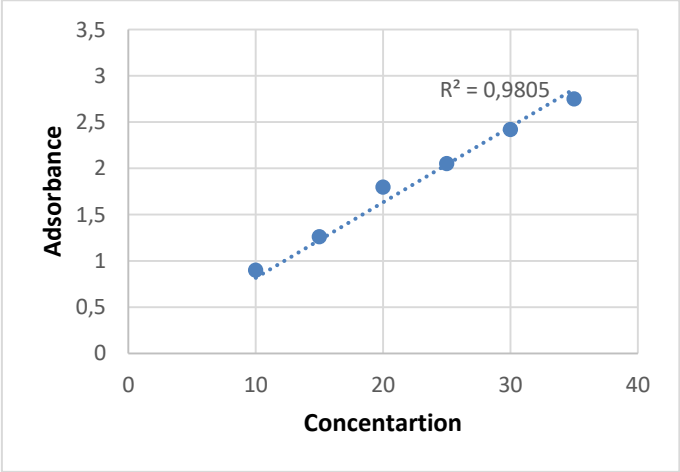

Figure 17. Samples with different contact time

Figure 18 shows the dye removal practically and by visual inspection as the color of the methyl orange has been removed and no orange color remains. The figure as well shows the degradation of the color according to the contact time between the dye (methyl orange) and the mixture of PVP with the metal ions.

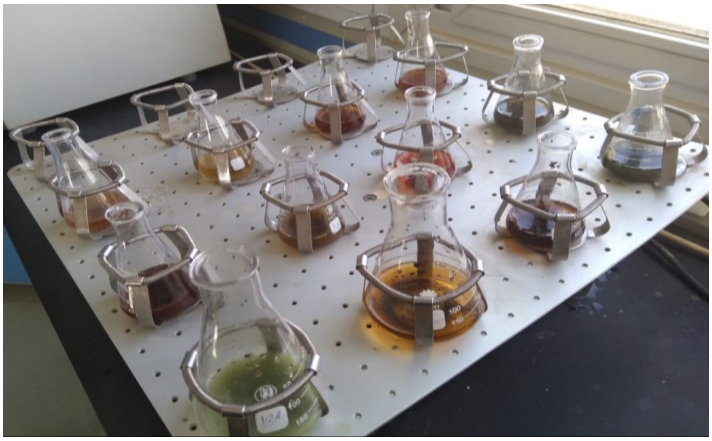

Figure 18. Contact Time Effect by shaking.

The figure shows same sample with same concentrations and the same mixture of PVP with metal ions but mixed with dye (methyl orange), the difference between them is the contact time between (10, 20, 30,40and 50 minutes). In order to get the best contact time between the dye and the mixture it should be held in a shaker with proper RPM. The resulted graphs show that the best curves were obtained from the nickel better than both ferric and copper. It also shows that ferric has the least proper curves because iron is known to have some problems when mixing with other chemical compounds based on previous experiments and articles. The graphs also show some errors in different points that lead not having a straight line that because of deactivating the catalyst as the catalyst adsorb the dye and after a certain time it does not keep the same amount adsorbed but it releases some amount of the dye in the solution again. The graphs show that by decreasing the amount of PVP weight and increasing the weight percent of the metal ions that lead to more dye removal.

The standard curve in Figure 17 shows the relation between concentrations and absorbance. The curve was obtained by applying different concentrations of methyl orange and obtains its absorbance. This curve makes the reading of concentrations more easily when applying the samples as the absorbance hit the curve and read the concentration. The curve gave R^2 =0.9805 which is acceptable.

4. CONCLUSIONS

An efficient method was adopted to generate a highly active nanoparticle based catalyst supported on graphene as ideal support. The Pd-Fe_3O_4/G catalyst was synthesized via using hydrothermal synthesis technique. Furthermore, the recovery and the recycling process of the catalyst could be implemented up to seven times with high catalytic activity near 100% thus providing high economic viability. It can be easily concluded from characterization that palladium nanoparticles and magnetite nanoparticles are uniformly dispersed onto the surface of graphene nanosheets.

This easy and efficient recycling process of the catalyst is simply due to the magnetic properties of magnetite, thus lead to achieving high yields over different substrates for Suzuki cross coupling reactions.

5. REFERENCES

1. Chen, S.T. Synthesis of Pd/Fe3O4 Hybrid Nanocatalysts with Controllable Interface and Enhanced Catalytic Activities for CO Oxidation. *Journal of Physical Chemistry C* **2012**, *116*, 12969-12976, https://doi.org/10.1021/jp3036204.
2. Radwan. N.R.E.; El-Shall, M.S.; Hassan, H.M.A. Synthesis and characterization of nanoparticle Co3O4, CuO and NiO catalysts prepared by physical and chemical methods to minimize air pollution. *Applied Catalysis A: General* **2007**, *331,* 8-18, https://doi.org/10.1016/j.apcata.2007.07.005.
3. Wang, H.L. Ni(OH)(2) Nanoplates Grown on Graphene as Advanced Electrochemical Pseudocapacitor Materials. *Journal of the American Chemical Society* **2010**, *132,* 7472-7477, https://doi.org/10.1021/ja102267j.
4. Wang, W.W.; Zhu, Y.J.; Ruan, M.L. Microwave-assisted synthesis and magnetic property of magnetite and hematite nanoparticles. J*ournal of Nanoparticle Research* **2007**, *9*, 419-426, https://doi.org/10.1007/s11051-005-9051-8.
5. Elazab, H. Microwave-assisted synthesis of Pd nanoparticles supported on FeO, CoO, and Ni(OH) nanoplates and catalysis application for CO oxidation. *Journal of Nanoparticle Research* **2014**, 16, 1-11, https://doi.org/10.1177/0263617418771777.
6. Mankarious R.A.; Radwan, M.A.; Shazly, M.; Elazab, H. Bulletproof vests/shields prepared from composite material based on strong polyamide fibers and epoxy resin. *Journal of Engineering and Applied Sciences* **2017**, *12*, 2697-2701.
7. Mohsen, W.; Sadek, M.A.; Elazab, H.A. Green synthesis of copper oxide nanoparticles in aqueous medium as a potential efficient catalyst for catalysis applications. *International Journal of Applied Engineering Research* **2017**, 12, 14927-14930.
8. Mostafa, A.R.; Omar, H.A.S.; Hany, A.E. Preparation of Hydrogel Based on Acryl Amide and Investigation of Different Factors Affecting Rate and Amount of Absorbed Water. *Agricultural Sciences* **2017**, *8*, 11, https://doi.org/10.4236/as.2017.82011.
9. Radwan, M.A.; Naeem, M.M.; Sadek, M.; Elazab, H. Mechanical characteristics for different composite materials based on commercial epoxy resins and different fillers. *Journal of Engineering and Applied Sciences* **2017**, *12*, 1179-1185.
10. Andrade, A.L. Catalytic Effect of Magnetic Nanoparticles Over the H(2)O(2) Decomposition Reaction. *Journal of Nanoscience and Nanotechnology* **2009**, *9*, 3695-3699, https://doi.org/10.1166/jnn.2009.ns53.
11. Kustov, A.L. CO methanation over supported bimetallic Ni-Fe catalysts: From computational studies towards catalyst optimization. *Applied Catalysis a-General* **2007**, *320,* 98-104, https://doi.org/10.1016/j.apcata.2006.12.017.
12. Lohitharn, N.; Goodwin, J.G. Impact of Cr, Mn and Zr addition on Fe Fischer-Tropsch synthesis catalysis: Investigation at the active site level using SSITKA. *Journal of Catalysis* **2008**, *257*, 142-151, https://doi.org/10.1016/j.jcat.2008.04.015.
13. Moreau, F.; Bond, G.C. CO oxidation activity of gold catalysts supported on various oxides and their improvement by inclusion of an iron component. *Catalysis Today* **2006**, *114*, 362-368, https://doi.org/10.1016/j.cattod.2006.02.074.
14. Sarkari, M. Fischer-Tropsch synthesis: Development of kinetic expression for a sol-gel Fe-Ni/Al2O3 catalyst. F*uel Processing Technology* **2012**, *97*, 130-139, https://doi.org/10.1016/j.fuproc.2012.01.008.
15. Elazab, H. The Effect of Graphene on Catalytic Performance of Palladium Nanoparticles Decorated with FeO, CoO, and Ni (OH): Potential Efficient Catalysts Used for Suzuki Cross-Coupling. *Catalysis Letters* **2017**, *147,* 1510-1522, https://doi.org/10.1007/s10562-017-1990-z.
16. Elazab, H.A. The continuous synthesis of Pd supported on Fe3O4 nanoparticles: A highly effective and magnetic catalyst for CO oxidation. *Green Processing and Synthesis* **2017,** 6, 413-424, https://doi.org/10.1515/gps-2016-0168.
17. Elazab, H.A.; Sadek, M.A.; El-Idreesy, T.T. Microwave-assisted synthesis of palladium nanoparticles supported on copper oxide in aqueous medium as an efficient catalyst for Suzuki cross-coupling reaction. *Adsorption Science & Technology* **2018**, https://doi.org/10.1177/0263617418771777.
18. Elazab, H.A. Highly efficient and magnetically recyclable graphene-supported Pd/Fe3O4 nanoparticle catalysts for Suzuki and Heck cross-coupling reactions. *Applied Catalysis A: General* **2015**, *491*, 58-69, https://doi.org/10.1016/j.apcata.2014.11.033.
19. Hirvi, J.T.; Kinnunen, T.J.; Suvanto, M.; Pakkanen, T.A.; Norskov, J.K. CO oxidation on PdO surfaces, *Journal of*

Chemical Physics **2010**, *133,* 8, https://doi.org/10.1063/1.3464481.
20. Iglesias-Juez, A. Nanoparticulate Pd Supported Catalysts: Size-Dependent Formation of Pd(I)/Pd(0) and Their Role in CO Elimination. *Journal of the American Chemical Society* **2011**, 133, 4484-4489, https://doi.org/10.1021/ja110320y.
21. Ivanova, A.S. Metal-support interactions in Pt/Al2O3 and Pd/Al2O3 catalysts for CO oxidation. *Applied Catalysis B-Environmental* **2010**, *97,* 57-71, https://doi.org/10.1016/j.apcatb.2010.03.024.
22. Kim, H.Y.; Henkelman, G. CO Oxidation at the Interface between Doped CeO2 and Supported Au Nanoclusters. *Journal of Physical Chemistry Letters* **2012**, *3*, 2194-2199.
23. Chattopadhyay, K.; Dey, R.; Ranu, B.C. Shape-dependent catalytic activity of copper oxide-supported Pd(0) nanoparticles for Suzuki and cyanation reactions. *Tetrahedron Letters: International Organ for the Rapid Publication of Preliminary Communications in Organic Chemistry* **2009**, *50*, 3164-3167, https://doi.org/10.1016/j.tetlet.2009.01.027.
24. Hoseini, S.J. Modification of palladium-copper thin film by reduced graphene oxide or platinum as catalyst for Suzuki-Miyaura reactions. *Applied Organometallic Chemistry* **2017**, *31,* https://doi.org/10.1002/aoc.3607.
25. Hosseini-Sarvari, M.; Razmi, Z. Palladium Supported on Zinc Oxide Nanoparticles as Efficient Heterogeneous Catalyst for Suzuki Miyaura and Hiyama Reactions under Normal Laboratory Conditions. *Helvetica Chimica Acta* **2015**, *98,* 805-818, https://doi.org/10.1002/hlca.201400331.
26. Nasrollahzadeh, M.; Ehsani, A.; Jaleh, B. Preparation of carbon supported CuPd nanoparticles as novel heterogeneous catalysts for the reduction of nitroarenes and the phosphine-free Suzuki Miyaura coupling reaction. *New Journal of Chemistry* **2015**, *39*, 1148-1153, https://doi.org/10.1039/C4NJ01788A.
27. Nasrollahzadeh, M. Palladium nanoparticles supported on copper oxide as an efficient and recyclable catalyst for carbon(sp2) carbon(sp2) cross-coupling reaction. *Materials Research Bulletin* **2013**, *68,* 150-154, https://doi.org/10.1016/j.materresbull.2015.03.051.
28. Mandali, P.K.; Chand, D.K. Palladium nanoparticles catalyzed Suzuki cross-coupling reactions in ambient conditions. *Catalysis Communications* **2016**, *31*, 16-20, https://doi.org/10.1016/j.catcom.2012.10.020.
29. Wang, Y. CuO Nanorods-Decorated Reduced Graphene Oxide Nanocatalysts for Catalytic Oxidation of CO. *Catalysts* **2016**, *6*, 214, https://doi.org/10.3390/catal6120214.
30. Igarashi, H.; Uchida, H.; Watanabe, M. Mordenite-supported noble metal catalysts for selective oxidation of carbon monoxide in a reformed gas. *Chemistry Letters* **2000**, *11,* 1262-1263, https://doi.org/10.1246/cl.2000.1262.
31. Liu, W.H.; Fleming, S.; Lairson, B.M. Reduced intergranular magnetic coupling in Pd/Co multilayers. *Journal of Applied Physics* **1996**, *79,* 3651-3655, https://doi.org/10.1063/1.361193.
32. Luo, J.Y. Mesoporous Co(3)O(4)-CeO(2) and Pd/Co(3)O(4)-CeO(2) catalysts: Synthesis, characterization and mechanistic study of their catalytic properties for low-temperature CO oxidation. *Journal of Catalysis* **2008**, *254,* 310-324, https://doi.org/10.1016/j.jcat.2008.01.007.
33. Pavlova, S.N. The influence of support on the low-temperature activity of Pd in the reaction of CO oxidation on Kinetics and mechanism of the reaction. *Journal of Catalysis* **1996**, *161,* 517-523, https://doi.org/10.1006/jcat.1996.0213.
34. Diyarbakir, S.M.; Can, H.; Metin, O. Reduced Graphene Oxide-Supported CuPd Alloy Nanoparticles as Efficient Catalysts for the Sonogashira Cross-Coupling Reactions. *Acs Applied Materials & Interfaces* **2015**, *7*, 3199-3206, https://doi.org/10.1021/am507764u.
35. Feng, Y.S.; Ma, J.J.; Kang, Y.M.; Xu, H.J. ChemInform Abstract: PdCu Nanoparticles Supported on Graphene: An Efficient and Recyclable Catalyst for Reduction of Nitroarenes. *ChemInform* **2015**, *70,* 6100-6105, https://doi.org/10.1016/j.tet.2014.04.034.
36. Feng. Y.S.; Ma, J.J.; Kang, Y.M.; Xu, H.J. PdCu nanoparticles supported on graphene: an efficient and recyclable catalyst for reduction of nitroarenes. *Tetrahedron* **2014**, *70*, 6100-6105, https://doi.org/10.1016/j.tet.2014.04.034.
37. Liu, Y.; Ma, H.; Wu, J.D.W.; Ren, X.; Yan, T.; Pang, X.; Wei, Q. Ultrasensitive electrochemical immunosensor for SCCA detection based on ternary Pt/PdCu nanocube anchored on three-dimensional graphene framework for signal amplification. *Biosensors & Bioelectronics* **2016**, *79*, 71-78, https://doi.org/10.1016/j.bios.2015.12.013.
38. Shafaei, D.A.; Saravani, H.; Noroozifar, M. Novel fabrication of PdCu nanostructures decorated on graphene as excellent electrocatalyst toward ethanol oxidation. *International Journal of Hydrogen Energy* **2017**, *42*, 15149-15159, https://doi.org/10.1016/j.ijhydene.2017.04.280.
39. Elazab, H.A. Investigation of Microwave-assisted Synthesis of Palladium Nanoparticles Supported on Fe_3O_4 as an Efficient Recyclable Magnetic Catalysts for Suzuki Cross – Coupling. *The Canadian Journal of Chemical Engineering* **2018**, *96*, 250-261, https://doi.org/10.1002/cjce.23402.
40. Radwan, M.A.; Omar Al-Sweasy, Sadek, M.A.; Elazab, H.A. Investigating the Agricultural Applications of Acryl Amide based Hydrogel. *International Journal of Engineering and Technology(UAE)* **2018**, *7*, 168-171.
41. Zakaria, F.; Radwan, M.A.; Sadek, M.; Elazab, H.A. Insulating material based on shredded used tires and inexpensive polymers for different roofs. *International Journal of Engineering and Technology(UAE)* **2018**, *7*, 1983-1988, https://doi.org/10.14419/ijet.v7i4.14081.
42. Nasser, R.; Radwan, M.A.; Sadek, M.A.; Elazab, H.A. Preparation of insulating material based on rice straw and inexpensive polymers for different roofs. *International Journal of Engineering and Technology(UAE)* **2018**, *7*, 1989-1994, https://doi.org/10.14419/ijet.v7i4.14082.
43. Ghobashy, M.; Gadallah, M.; El-Idreesy, T.T.; Sadek, M.A.; Elazab, H.A. Kinetic Study of Hydrolysis of Ethyl Acetate using Caustic Soda. *International Journal of Engineering and Technology(UAE)* **2018,** *7*, 1995-1999, https://doi.org/10.14419/ijet.v7i4.14083.
44. Samir, N.S.; Radwan, M.A.; Sadek, M.A.; Elazab, H.A. Preparation and Characterization of Bullet-Proof Vests Based on Polyamide Fibers. *International Journal of Engineering and Technology(UAE)* **2018**, *7*, 1290-1294, https://doi.org/10.14419/ijet.v7i3.13175.
45. Ashraf, B.; Radwan, M.A.; Sadek, M.A.; Elazab, H.A. Preparation and Characterization of Decorative and Heat Insulating Floor Tiles for Buildings Roofs. *International Journal of Engineering and Technology (UAE)* **2018**, *7*, 1295-1298, https://doi.org/10.14419/ijet.v7i3.13177.
46. Mandali, P.K.; Chand, D.K. Palladium nanoparticles catalyzed Suzuki cross-coupling reactions in ambient conditions. *Catalysis Communications* **2016**, *31*, 16-20, https://doi.org/10.1016/j.catcom.2012.10.020.
47. Elazab, H. Investigation of Microwave-assisted Synthesis of Palladium Nanoparticles Supported on Fe3O4 as an Efficient Recyclable Magnetic Catalysts for Suzuki Cross – Coupling. *The Canadian Journal of Chemical Engineering* **2019**, *97*, 920-928, https://doi.org/10.1002/cjce.23402.
48. Radwan, M.A.; Rashad, M.A.; Sadek, M.A.; Elazab, H.A. Synthesis, Characterization and Selected Application of Chitosan Coated Magnetic Iron Oxide Nanoparticles. *Journal of Chemical Technology and Metallurgy* **2019**, 54, 303-310.

49. Abdelhady, H.H.; Elazab, H.A.; Ewais, E.M.; Saber, M.; El-Deab, M.S. Efficient Catalytic Production of Biodiesel Using Nano-Sized Sugarbeet Agro-Industrial waste. *Fuel* **2019**, Accepted, https://doi.org/10.1016/j.fuel.2019.116481.
50. Elazab, H.A. Investigation of Microwave-assisted Synthesis of Palladium Nanoparticles Supported on Fe_3O_4 as an Efficient Recyclable Magnetic Catalysts for Suzuki Cross – Coupling. *The Canadian Journal of Chemical Engineering* **2019**, *97*, 1545-1551, https://doi.org/10.1002/cjce.23402.
51. Elazab, H.A.; Sadek, M.A.; El-Idreesy, T.T. Facile Synthesis of Reduced Graphene Oxide-Supported Pd/CuO Nanoparticles as an Efficient Catalyst for Cross-Coupling Reactions. *Journal of Chemical Technology and Metallurgy* **2019**, *54*, 934-946.
52. Elazab, H.A.; El-Idreesy, T.T. Polyvinylpyrrolidone - Reduced Graphene Oxide - Pd Nanoparticles as an Efficient Nanocomposite for Catalysis Applications in Cross-Coupling Reactions. *Bulletin of Chemical Reaction Engineering and Catalysis* **2019**, *14,* 490-501, https://doi.org/10.9767/bcrec.14.3.3461.490-501.
53. Elazab, H.A.; Ali, R.; Siamaki, B.; Gupton, F.; El-Shall, M.S. Pd-Fe_3O_4/RGO: a Highly Active and Magnetically Recyclable Catalyst for Suzuki Cross Coupling Reaction using a Microfluidic Flow Reactor. *Bulletin of Chemical Reaction Engineering and Catalysis* **2019**, *14,* 478-489, https://doi.org/10.9767/bcrec.14.3.3518.478-489.
54. Elazab, H.A.; Radwan, M.A.; El-Idreesy, T.T. Facile microwave-assisted synthetic approach to palladium nanoparticles supported on copper oxide as an efficient catalyst for Heck cross-coupling reactions. *International Journal of Nanoscience* **2019**, *18*, 1850032, https://doi.org/10.1142/S0219581X18500321.
55. Elazab, H.A.; Hassan, S.A.; Radwan, M.A.; Sadek, M.A. Microwave-assisted Synthesis of Graphene supported Hexagonal Magnetite for Applications in Catalysis. *International Journal of Innovative Technology and Exploring Engineering (IJITEE)* **2019**, *8*, 5511-5513.
56. Elazab, H.A.; Radwan, M.A.; Sadek, M.A. Hydrothermal Synthesis of Palladium nanoparticles supported on Fe_3O_4 Nanoparticles: an Efficient Magnetic Catalysts for CO Oxidation. *International Journal of Innovative Technology and Exploring Engineering (IJITEE)* **2019**, *8*, 2792-2794, https://doi.org/10.33263/BRIAC92.906911.
57. Aboul-Fotouh, T.M.; Sherif, K.; Ibrahim, M.A.; Sadek, M.A.; Elazab, H.A. High Octane Number Gasoline-Ether Blend. *International Journal of Innovative Technology and Exploring Engineering (IJITEE)* **2019**, *8,* 732-739,
58. Aboul-Fotouh, T.M.; Alaa, I.; Sadek, M.A.; Elazab, H.A. Physico-Chemical Characteristics of Ethanol–Diesel Blend Fuel. *International Journal of Innovative Technology and Exploring Engineering (IJITEE)* **2019**, *8*, 740-747.
59. Elazab, H.A.; Seleet, M.M.; Said, M.A.; Hassanein, M.A.; Radwan, M.A.; Sadek, M. Synthesis and Characterization of Dinitro Pentamethylene Tetramine (DPT). *Journal of Advanced Research in Dynamical and Control System* **2019**, *11*, 310-318.
60. Elazab, H.A.; Seleet, M.M.; Said, M.A.; Hassanein, M.A.; Radwan, M.A.; Sadek, M. Follow-up and Kinetic Model Selection of Dinitro Pentamethylene Tetramine (DPT). *International Journal of Innovative Technology and Exploring Engineering (IJITEE)* **2019**, *8*, 2862-2866.
61. Elazab, H.A.; Seleet, M.M.; Said, M.A.; Hassanein, M.A.; Radwan, M.A. Sadek, M. 3,7-Dinitro-1,3,5,7-Tetraazabicyclo[3,3,1]Nonane (DPT): An Important Intermediate in the Synthesis Route of one of the Most Powerful Energetic Materials (RDX/HMX). *International Journal of Innovative Technology and Exploring Engineering (IJITEE)* **2019**, *8*, 88-95.

6. ACKNOWLEDGEMENTS

We express our deep gratitude to British University in Egypt (BUE). This work was partially performed using the facilities at the Nanotechnology Research Centre (NTRC) at the British University in Egypt (BUE).